

COB-2023-0188
**FREQUENCY POWER LAWS FOR THE DECAY OF THE LEAK
NOISE SPECTRUM IN SANDY SOIL WITH DIFFERENT DEGREES
OF COMPACTION**

Matheus Silva Proença
Daniel Henrique de Sousa Obata
Amarildo Tabone Paschoalini
Vinícius de Araújo Salmazo

São Paulo State University (UNESP) – School of Engineering, Ilha Solteira, SP, Brasil.
matheus.proenca@unesp.br, daniel.obata@unesp.br, amarildo.tabone@unesp.br, vinicius.salmazo@unesp.br

Abstract. Leaks in urban water distribution networks are still a great challenge for several supply companies around the world, and, in this scenario, the vibro-acoustic detection/location techniques have stood out as part of the problem's solution. However, some factors, such as the geological environment and its compaction, affect the measurement of the leakage signal on the ground surface and, consequently, harm the efficiency of these techniques. Therefore, this manuscript was carried out to numerically investigate the influence of the degrees of compaction of sandy soils upon its power laws of attenuation. The sandy soil was modeled as a viscoelastic solid using a previously validated Kelvin–Voigt model, and the differential equations describing the problem were solved using the Finite Element Method (FEM). The results showed that the frequency-dependent attenuation obeys a specific power law for each degree of compaction of the sandy soil. It has been found that the leak noise spectra decay with a frequency power law close to $1/\omega^2$ in the soil with a controlled compaction level and equal to $1/\omega$ in the soil with a high compaction level. Furthermore, in an experimental test, an inverse method was applied to predict the temporal signal of an excitation source at the base of a sand massif using only the experimental output signal measured on the ground surface and its calculated numerical attenuation. The compared results agreed very well.

Keywords: Frequency power law, Soil attenuation, Soil compaction, Viscoelasticity.

1. INTRODUCTION

Although water losses are inherent to any supply system, in several countries, supply companies still face worrying loss rates. In Brazil, for instance, approximately 40% of treated water is lost, on average, in underground distribution networks (SNIS, 2022) and around 60% of this volume is essentially due to leaks in the networks (GO-Associates and Trata Brasil Institute, 2021). To combat this serious problem, advances in leak detection/location methods have been occurring in recent years and among the techniques applied in the water industry, the vibro-acoustic methods stand out (Tsujiya, 2008) for having good sensitivity and accuracy, lower false alarm rate and shorter work time (Liu *et al.*, 2017).

The vibro-acoustic methods, through convenient instrumentation, detect the signal of the leak's noise that propagates from underground to the surface of the massif or at pipe access points, such as fire hydrants and valves. However, some factors, such as the existing geological environment and the compaction performed during the backfilling of the ditches, affect the measurement of this signal on the ground surface and, consequently, the efficiency of these methods.

In this way, the present work aims to contribute to this scenario by investigating the influence of the degrees of compaction of sandy soil upon frequency power laws of the material damping in a finite frequency band, promising for the vibro-acoustic detection of leaks. Knowing the attenuation behavior of the soil around the pipeline and its leakage is a significant step to determining the noise characteristics of the leak at the source, assisting in analytical and numerical approaches and in the application of vibro-acoustic methods that remotely measure the buried leak.

As mentioned by Scussel *et al.* (2021), in practice, it is difficult to measure leak noise at the source, so an inverse method using measurements made on the ground surface should stand out in these predictions. Frequently, the spectrum of the leaks at the source can be represented by white noise, however, there is still very little data to better consolidate this assumption. In this way, the present work aims to contribute to this gap too.

The investigations made in the manuscript started from numerical analysis, in which sandy soil with different degrees of compaction was modeled as a visco-elastic solid using the Kelvin-Voigt model previously studied and experimentally validated by Proença *et al.* (2022). The differential equations that describe the problem, Eq. (1), were solved by applying the Finite Element Method (FEM).

This paper is organized as follows. Following this introduction, Section 2 describes the numerical modeling and procedures adopted for the simulation of the sandy soil and its degrees of compaction. Exposure and discussion of the results are given in Section 3 and some conclusions are given in Section 4.

2. METHODOLOGY

2.1 Numerical approach

The complex behavior of geomaterials depends both on their nature and on their state - humidity, degrees of compaction, etc. -, as well as external parameters, such as the amplitude and frequency of the excitation, stress loading profile, and their time duration (Pinto, 2006). Researchers (Di Benedetto and Tatsuoka, 1997) classified soils into four different domains according to their level of deformation. For low deformations, eg. in the order of 10^{-5} m/m, the behavior of soils can be considered almost linear elastic. Then, Proença *et al.* (2022) verified that the non-conservative forces of this problem can be conveniently simulated through a linear visco-elastic model.

Therefore, this work has presented an approach based on Kelvin-Voigt visco-elastic model to simulate the response of a sandy soil to a buried point source vibration. Proença *et al.* (2022) describe in detail the development of this applied model. The numerical model is representative of the response of the soil to small excitations such as underground water leaks and was already validated experimentally for the sandy soil addressed.

The Finite Element Method was used to solve the partial differential equations describing the motion of the two-dimensional, isotropic, linear visco-elastic solid – Eq. (1). The problem's geometry was discretized using isoparametric, two-dimensional, 4-nodes elements, and 2 degrees of freedom per node, which are the displacements in y and z directions. The work assumed the plane stress state, with the equations of motion derived in the plane perpendicular to the pipe axis.

$$\rho \cdot \frac{\partial^2 v}{\partial t^2} = \left\{ \left(\frac{E}{1-\nu^2} \right) \cdot \left[\frac{\partial^2 v}{\partial y^2} + \eta^* \cdot \frac{\partial^3 v}{\partial y^2 \partial t} + \nu \cdot \left(\frac{\partial^2 w}{\partial y \partial z} + \eta^* \cdot \frac{\partial^3 w}{\partial y \partial z \partial t} \right) \right] \right\} + \left\{ G \cdot \left[\frac{\partial^2 v}{\partial z^2} + \frac{\partial^2 w}{\partial y \partial z} + \eta^* \cdot \left(\frac{\partial^3 v}{\partial z^2 \partial t} + \frac{\partial^3 w}{\partial y \partial z \partial t} \right) \right] \right\} \quad (1a)$$

$$\rho \cdot \frac{\partial^2 w}{\partial t^2} = \left\{ \left(\frac{E}{1-\nu^2} \right) \cdot \left[\frac{\partial^2 w}{\partial z^2} + \eta^* \cdot \frac{\partial^3 w}{\partial z^2 \partial t} + \nu \cdot \left(\frac{\partial^2 v}{\partial y \partial z} + \eta^* \cdot \frac{\partial^3 v}{\partial y \partial z \partial t} \right) \right] \right\} + \left\{ G \cdot \left[\frac{\partial^2 w}{\partial y^2} + \frac{\partial^2 v}{\partial y \partial z} + \eta^* \cdot \left(\frac{\partial^3 w}{\partial y^2 \partial t} + \frac{\partial^3 v}{\partial y \partial z \partial t} \right) \right] \right\} + b_z(y, t) - \rho \cdot g \quad (1b)$$

where ρ is soil density, E is Young's modulus, ν is the Poisson's ratio, G is the shear modulus, and $\eta^* = \eta/E$ is the retardation time, ratio between the materials viscous damping ratio, η , and its elastic properties. While v and w are displacements in y and z direction, respectively, g is acceleration due to gravity, and b_z is a force exciting the base of the plane per unit area.

The Newmark implicit integration method was used to discretize the governing equations in the time domain, and the approach of the weak formulation of these equations was applied for the space integration, thus reducing the order of the equations. The system of discretized equations was solved using the Generalized Minimal Residual Method (GMRES), and at each time step, the admissibility of the elastic predictor was verified using the Mohr–Coulomb yield criterion. All the numerical simulation of the work was developed in MATLAB software.

Figure 1 shows the representation of the problem and the adopted boundary conditions.

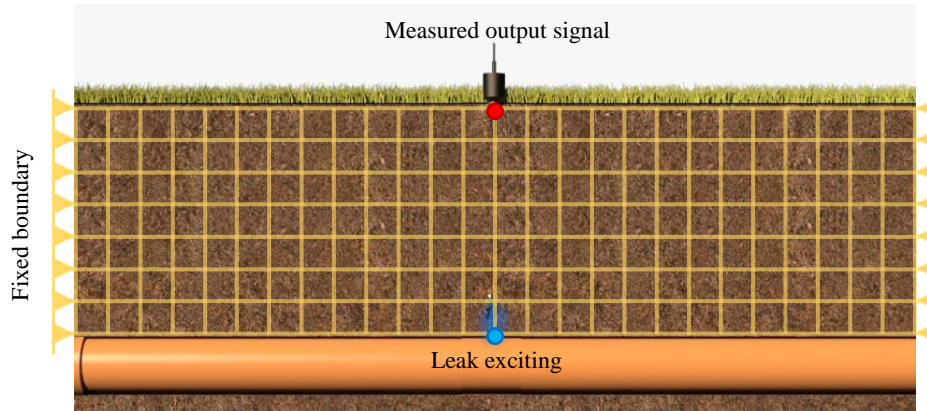


Figure 1. Illustration of the model.

As represented in Figure 1, the horizontal boundary is fixed, therefore, in $y = 0$ and $y = L$, $v(z, t) = w(z, t) = 0$. Further, in the bottom boundary, there is a prescribed acceleration $a_b(y, 0, t) = \ddot{w}_b(y, 0, t)$, in the central node of the material's base, because the leak was simulated as a point source of vertical vibration.

The numeric mesh was generated and refined in the pre-processing step of the developed algorithm itself. The solution's convergence was tested from the root mean square acceleration of one superficial node and it was selected finite elements with a size equal to 9.1 mm, thus, the 0.4 m soil layer was discretized with 2904 elements (66 x 44 mesh).

Materials' frequency-dependent attenuation is observed in a wide range of important engineering areas (Chen and Holm, 2004), including studies on soils dynamics. In this work, the soil attenuation is given by.

$$att(\omega) = -20 \cdot \log_{10}(|H_{xy}(\omega)|) \quad (2)$$

where $H_{xy}(\omega)$ is the Frequency Response Function (FRF), ratio between the cross and auto-power spectrum density of excitation signal and the ground surface acceleration, in a point right up the excitation point.

$$H_{xy}(\omega) = \frac{S_{xy}(\omega)}{S_{xx}(\omega)} \quad (3)$$

Then, the attenuation of the leak signal that propagates along the massif may be correlated with a power law distribution as follows.

$$att(\omega) \approx \beta \cdot \omega^\alpha, \quad \alpha \in [0,2], \quad (4)$$

The media-specific attenuation parameters, β and α , are obtained through a fitting of the processed data. Such a procedure is usually done on a plot in log-log coordinates, as can be seen in Figure 2b, allowing a simple linear function to represent the increase of the material's damping with the frequency, over a finite bandwidth predetermined (Pritz, 2004). The exponent of the expression is a positive number and typically less than 2 (Chen and Holm, 2004).

In a classical solution for a simple one-dimensional case, for instance, the amplitude of an output signal could be described by a relation as follows.

$$A(x + \Delta x) = A(x) \cdot e^{-att(\omega) \cdot \Delta x} \quad (5)$$

where A denotes the amplitude of an acoustic field variable, and Δx is wave propagation distance.

As discussed by Pritz (2004), the attenuation, $att(\omega)$, is closely linked with the loss modulus of the dynamic complex modulus of a material, ie. the negative imaginary part of the wave number k . For instance, taking as reference the complex Young's modulus E^* we have.

$$E^*(j\omega) = E_d(\omega) + j \cdot E_l(\omega); \quad \text{and} \quad E_l(\omega) = att(\omega) = \beta \cdot \omega^\alpha \quad (6)$$

where $j = \sqrt{-1}$ is the imaginary unit, E_d is the dynamic modulus of elasticity, E_l is the loss modulus. The dynamic elastic and damping properties of solid materials are characterized in many studies in the frequency domain through this concept of complex modulus of elasticity.

For small deformations ($\varepsilon < 10^{-5}$), as occurs in the present work, the dispersion of the dynamic modulus is negligibly small, so $E_d(\omega) \approx E_0$, and this regardless of the type and status of soil (Sun, Goleosorkhi and Seed, 1988; *apud* Proença, 2019). For low-loss materials, the dynamic modulus can also be considered almost frequency independent, while both the loss modulus and loss factor may exhibit a frequency increase (Pritz, 2004).

Then, frequency power laws has been suggested in this work to describe the increase of damping experienced for sandy soils over a finite bandwidth related to the promising frequency range for the detection of underground water leaks.

2.2 Sandy soil compaction and its properties

Due to the importance that the compaction process has for the suitable settlement of pipes in ditches – avoiding stress concentrations and unwanted bending moments (El Debs, 2003) – there are in the country several normative guidelines to be followed by water supply companies (NBR 5626 - ABNT, 2020; NBR 17015 - ABNT, 2022). In the field, the compaction stage is usually carried out in layers, and the equipment used varies according to the occasion (NBR 17015 - ABNT, 2022).

Dealing with three-phase materials, the compaction of the soils generates a rearrangement of its solid particles, reducing pore space between them, while eliminating air/water that were contained there (Pinto, 2006). This process directly affects the homogeneity, density, and elastic and viscous stiffness of the soil, and, consequently, its dynamic response, as well as the velocity of waves' propagation in it. Thus, in this work, for each degree of compaction practiced, we will have different values for the elastic and viscous properties of the sandy soil.

The Standard Penetration Test (SPT) is a simple, cheap, and widely applied test *in-situ*, which is based on the resistance to penetration of the massif. This test basically consists of counting the number of blows (N_{SPT}) needed for a standardized sampling tube penetrating a layer of 0.15 m (Pinto, 2006). This dynamic penetration test was designed to provide some information on the geotechnical engineering properties of soils.

Then, with a representative set of experimental data, the researchers Ohsaki and Iwasaki (1973) empirically related the shear modulus (G) with the Penetration Resistance Index (N_{SPT}) of several soils. From these empirical studies, following the expression obtained for sandy soils.

$$G = 6.37 \times 10^6 \cdot N_{SPT}^{0.94} \text{ [Pa]} \quad (7)$$

Knowing the Poisson's ratio (ν) of the worked soil, which can generally vary in the range of [0.30 - 0.50], it is also possible to relate, approximately, the Modulus of Elasticity (E) with the N_{SPT} number, applying the Eq. (7) in (8)

$$E = 2 \cdot G \cdot (1 + \nu) \quad (8)$$

In Brazil, the Brazilian Association of Technical Standards (ABNT), in standard NBR 6484, prescribes technical information on soil drilling (2020). All compaction levels used in the numerical simulations in the present work, related to penetration resistance index, N_{SPT} , were selected from this standard. Thus, the influence of 5 degrees of compaction on the spectral characteristics of the water leakage signal that propagates from the subsoil to the surface of the sandy massif was investigated.

First, the water leakage was simulated as a point source of vertical vibration in the center of the material's base from a swept sine input, within the frequency range $\omega = [300 - 800]$ Hz over which leak noise is detected by sensors.

For the numeric implementations, the modulus G and E were calculated by Eq. (7) and (8), respectively. Moreover, the Poisson's ratio $\nu = 0.40$, the soil density (ρ) varied in the range of [1800 - 2000] kg/m³, depending on the degree of compaction, as shown in Tab.1, and the retardation time took on a constant value $\eta^* = 5.40 \times 10^{-5}$ s. At last, to ascertain whether the elastic predictor is admissible ($F < 0$), ie. if the stress state not reaches or exceeds the plasticity threshold as developed by Proença *et al.* (2022), the cohesion $c = 1$ kPa, and the angle of internal friction $\phi = 35^\circ$.

3. RESULTS AND DISCUSSION

The five arrangements used in the numerical implementations of the sandy soil are presented in Table 1.

Table 1. Arrangements used in numerical implementations of sandy soil.

Compaction level	Penetration resistance index [N_{SPT}]	Density [kg/m ³]
Very loose	2	1800
Loose	6	1900
Medium	13	1900
Dense	27	2000
Very dense	41	2000

Then, Figure 2a shows the numeric attenuation obtained for each degree of compaction, and Figure 2b shows, as an example, the calculation of the correlation exponents β and α through the log-log relationship, in the case with $N_{SPT} = 2$. A linear regression line was fitted to the presented data. The results show that the attenuation of the leak noise that propagates along the sandy soil follows a specific frequency power law for each degree of compaction of the massif. Table 2 gathers the parameters calculated for all cases.

In the physical interpretation of problems described through power laws, the correlation exponent has great importance (Bashan *et al.*, 2008; Zheng, Song and Wang, 2008; Galhardo *et al.*, 2009). For instance, the exponent $\alpha \approx 1.50$ suggests that the signal power spectral density decays with a frequency power law close to $1/\omega^2$. Thus, in this condition, the power density decreases 6 dB per octave and 20 dB per decade with increasing frequency. This case was observed in marginally compacted soils. While the exponent $\alpha \approx 1$, noted in soils with good compaction, suggests that the leak signal power spectral density decays with a frequency power law proportional to $1/\omega$. In this condition the power density decreases 3 dB per octave and 10 dB per decade with increasing frequency.

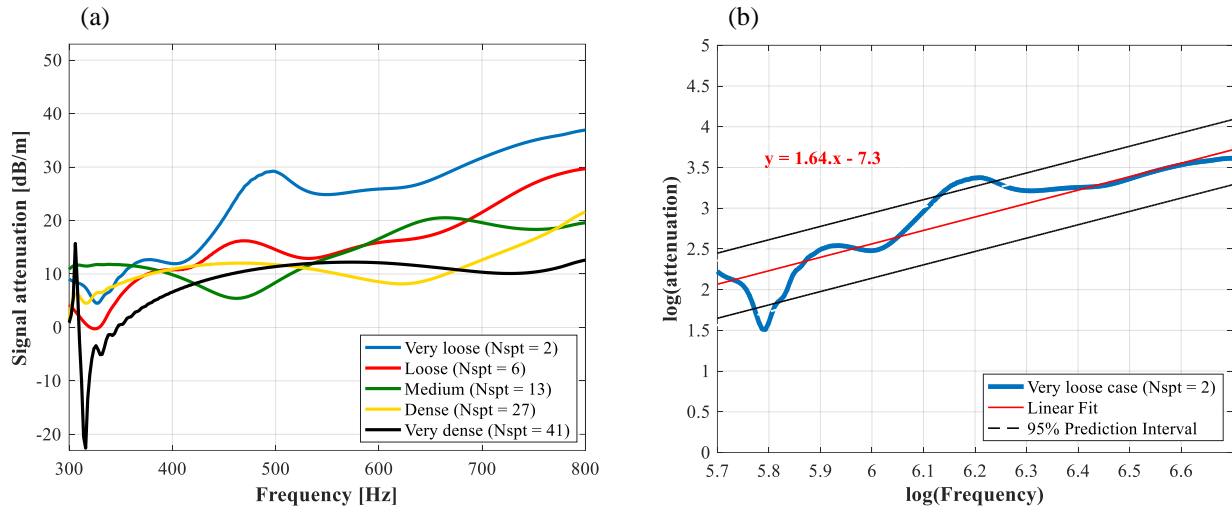


Figure 2. a) Signal attenuation for each degree of compaction of the sandy soil. b) Allometric relationship between attenuation and excitation frequency ($N_{SPT} = 2$).

Therefore, if the signal emitted by an underground leak is treated as a white noise, it can be said that on the surface of sandy soil with a loose compaction level the sensors will measure a signal similar to a Brownian noise, while on the surface of the soil with high compaction level will be found a pink noise. Other works in geophysics applied the power law, especially with $\alpha \approx 1$, to absorption in rock layers, as reviewed by Aki and Richards (1980, *apud* Szabo, 1994).

Figure 3 shows the frequency power laws obtained from the fit procedures of the curves of numeric attenuation, for each degree of compaction that was implemented.

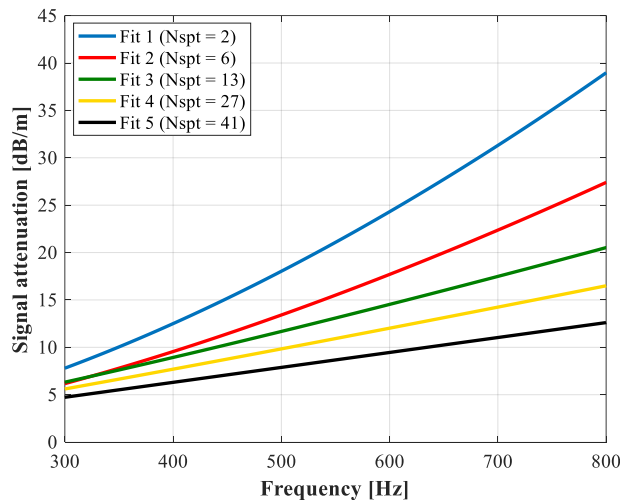


Figure 3. The leak signal attenuation: frequency power laws resulting from the fit procedures.

With varying the degrees of compaction, the studied soil presented two different behaviors. By the classification discussed by Galhardo *et al.* (2009), the sandy soil with a controlled compaction level tends to follow a diffusive behavior, by presenting $\alpha \approx 1.50$, while with the section with $\alpha < 1.50$, the soil with a high compaction level tends to adopt a subdiffusive behavior. Table 2 lists the attenuation parameters β and α found for each degree of compaction.

Table 2. The attenuation parameters β and α for the study cases.

Compaction level	β	α
Very loose	6.70×10^{-4}	1.64
Loose	1.10×10^{-3}	1.52
Medium	6.70×10^{-3}	1.20
Dense	1.06×10^{-2}	1.10
Very dense	1.58×10^{-4}	1.00

Then, using the frequency power laws obtained from seven different degrees of compaction, we built up a representative polynomial surface that encapsulates the result of fitting the model, predicting the attenuation level for each Penetration Resistance Index (N_{SPT}) in any frequency of the band of interest. The fit was made by the least squares method. For good conditioning, the input data was previously normalized.

As shown in Figure 4a, a surface with degree 2 in the frequency and degree 4 in the N_{SPT} was found. Figure 4b shows the error associated with fitting this surface to known attenuation curves. The maximum absolute error obtained was 19.69%, and the mean absolute error was 2.76%.

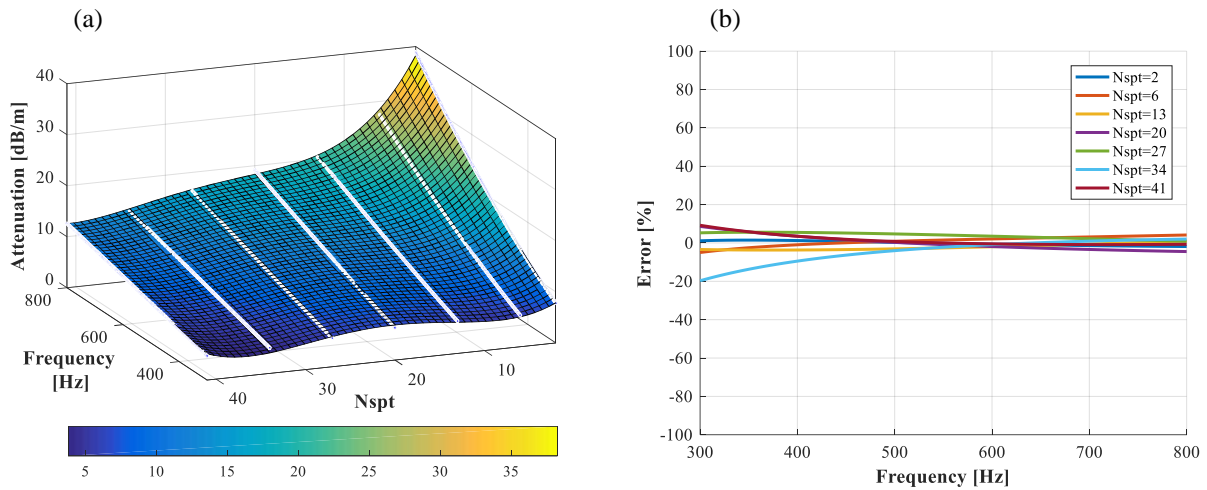


Figure 4. a) Representative polynomial surface for the signal attenuation. b) Error associated with predictions.

It must be emphasized that the proposed models for frequency power laws are assumed to be valid only over the bandwidth that was addressed, because, as mentioned by Pritz (2004), the viscoelastic materials can assume different behaviors in other frequencies. Therefore, these models will no longer be suitable for these other frequency bands. In addition, parameters such as the soil type and your physical state – not only the degree of compaction but also humidity, homogeneity, etc. – as well as the source characteristics – compression/shear – can influence and change the allometric relationships. These effects should also be further studied.

As already mentioned, knowing the attenuation behavior of the worked soil is a significant step toward determining the characteristics of the leak at the source. In practice, it is difficult to measure this noise of the underground source; therefore, an inverse method using the numeric results on the ground surface could assist this, collaborating with others' analytical and numerical approaches and with improvements in the leak detection/localization process through vibro-acoustic methods that measure the buried leak on the ground surface.

In this way, based on the presented findings and applying the fundamentals discussed in Section 2.1, it was possible to predict the excitation signal of a source at the base of a massif of sand through a signal experimentally measured by an accelerometer on the ground surface. Figure 5 shows the experimental test.

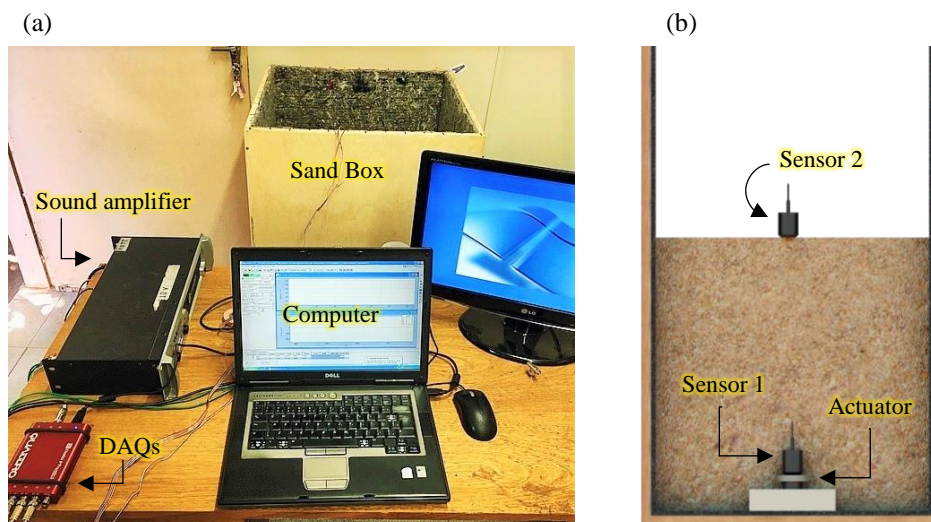


Figure 5. a) Experimental setup. b) Representation of the plywood box and the instrumentation.

The experimental setup was composed of a plywood box with dimensions of $0.6 \times 0.6 \times 1.0$ m ($L \times W \times D$), inner-covered with a 10-mm-thick soft polyester mantle, and filled with a medium-fine compacted sand, which was previously air-dried and sieved. The leak was simulated in the center of the bottom of the box through an electromechanical actuator installed in an expanded polyethylene (EPE) foam-made cradle to avoid wave transmission through the base of the box. The generated input signal was a white noise in the range [0-1000] Hz. An accelerometer was also fixed to the actuator to monitor this signal and compare it with the predicted signal.

Signal acquisition was carried out with one laptop computer, one Data Physics Quattro acquisition system (DAQs), one Crown XLS1000 sound amplifier and uniaxial piezoelectric accelerometers PCB 333B at a 4096 Hz sampling frequency. For the test, the thickness of the sand layer was 0.45 m.

Finally, Figure 6a shows the FFT of the signals collected at the base (input) and on the ground surface (output), while Figure 6b compares the module of the experimental Frequency Response Function, obtained by Eq. (3) and the numerical FRF obtained from the polynomial surface for the signal attenuation, for an $N_{SPT} = 7$. Eq. (2) gives

$$|H_{num}(\omega)| = 10^{-att(N_{SPT}, \omega)/20} \quad (9)$$

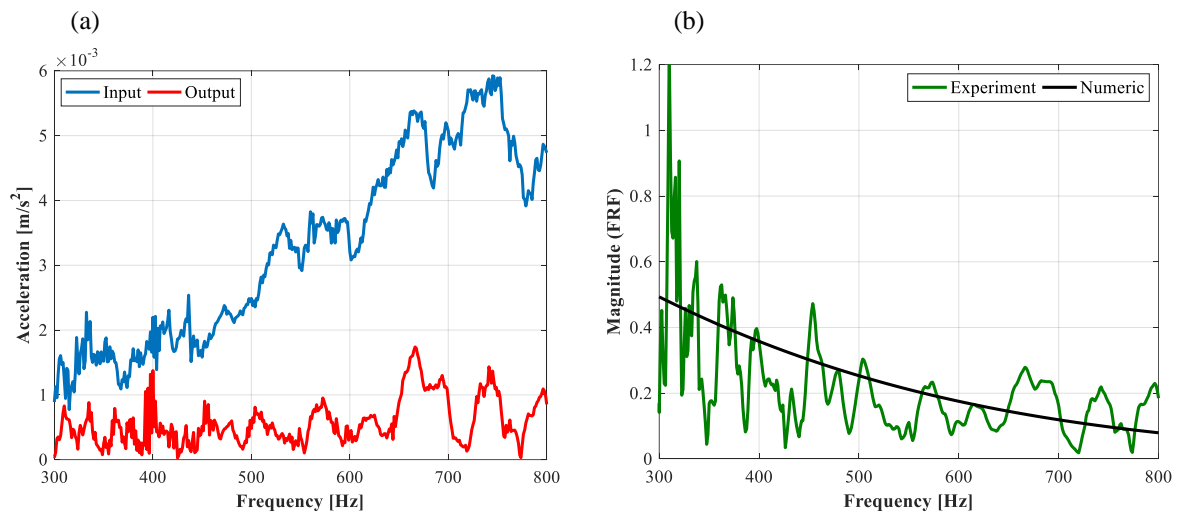


Figure 6. a) Fast Fourier Transform of the input and output signals. b) Experimental and numerical FRF.

As expected, the compared results agree very well. Then, the input signal of the leak in the frequency domain, $X(\omega)$, was reconstructed from the signal collected on the ground surface, $Y(\omega)$, as follows

$$X(\omega) = |2 \cdot Y(\omega)| \cdot \left(\frac{1}{|H_{num}(\omega)|} \right) \quad (10)$$

As there is no phase correction information in the field, the original temporal signal, $x(t)$, is not perfectly recoverable. However, it is possible to create a random time series with the same spectral characteristics as the original signal. In this way, before carrying out the inverse transform of $X(\omega)$, it was multiplied by a perfect white noise with a random phase in the frequency domain and $rms = 1$. For the manipulation, $X(\omega)$ needs to have a double-sided spectrum. A bandpass filter was also applied in the interval of interest.

$$x(t) = \text{real} \left[iFFT \left(X(\omega) \cdot \text{noise}(\omega) \cdot \text{filter}(\omega) \right) \right] \quad (11)$$

Figure 7a compares the original signal of the leak with the reconstructed signal, in the frequency domain, and the findings show good agreement between the data. Finally, Figure 7b presents the generated signal $x(t)$.

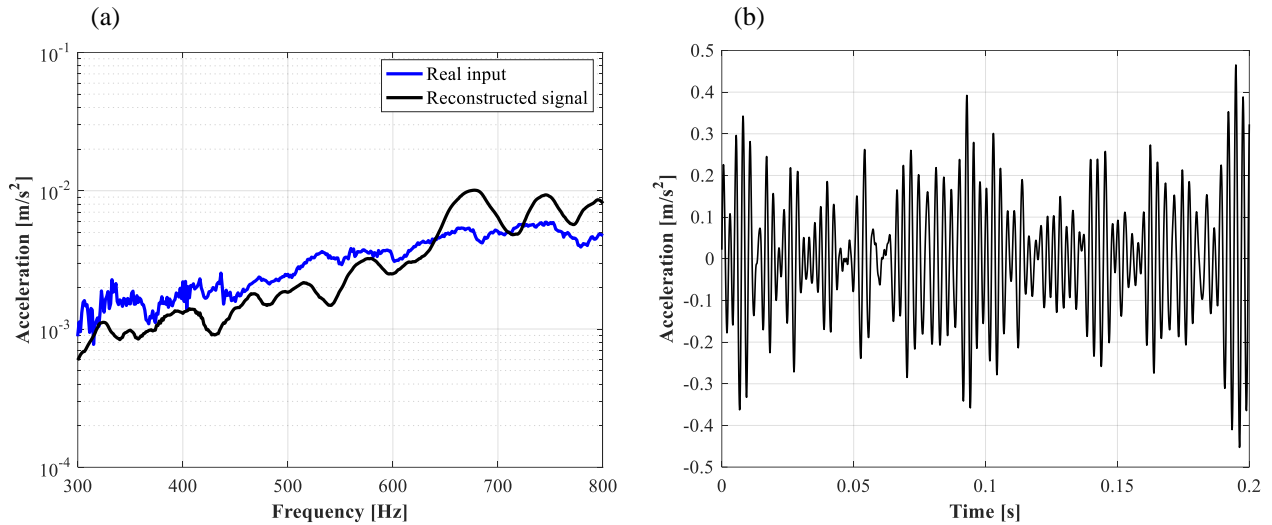


Figure 7. a) Comparison between the original signal and the reconstructed signal of the leak in the frequency domain. b) Signal of the leak in time domain, $x(t)$.

4. FINAL REMARKS

Comprehending the attenuation behavior of the soil around a pipeline and its leakage is an important step to determining the noise characteristics of the leak at the source, assisting in the improvement of researches in this area and of vibro-acoustic methods that remotely measure the buried leak. Thus, the present manuscript modeled a sandy soil with different degrees of compaction through the viscoelastic Kelvin–Voigt model.

The frequency-dependent attenuation of the geomaterial obeys a specific power law for each degree of compaction, thus, a representative polynomial surface was built in the work to predict the attenuation level for each Penetration Resistance Index (N_{SPT}) in any frequency of the band of interest. The findings showed that in the soil with a controlled compaction level and it with a high compaction level, the leak noise spectra decay with a frequency power law close to $1/\omega^2$ and $1/\omega$, respectively.

At last, in an experimental test, the temporal signal of an underground source on the base of a massif of sand was predicted using only the experimental output signal measured on the ground surface and the numeric attenuation calculated for it. The applied inverse method showed good results in the prediction, and can be used to describe in greater detail the signal of an underground leak.

5. ACKNOWLEDGEMENTS

The authors disclosed receipt of the following financial support for the research, authorship, and/or publication of this article: This work was supported by the Coordination for the Improvement of Higher Education Personnel (CAPES).

6. REFERENCES

- ABNT (Brazilian Association of Technical Standards), 2022. *NBR 17015: Execution of linear works for the transport of raw and treated water, sewage and urban drainage, using rigid, semi-rigid and flexible pipes* (in Portuguese). Rio de Janeiro, pp. 114.
- ABNT (Brazilian Association of Technical Standards), 2020. *NBR 5626: Building systems of cold water and hot water - Design, execution, operation and maintenance* (in Portuguese). Rio de Janeiro, pp. 56.
- ABNT (Brazilian Association of Technical Standards), 2020. *NBR 6484: Soil – Simple Reconnaissance Soundings with SPT – Testing Method* (in Portuguese). Rio de Janeiro, pp. 28.
- Aki, K. and Richards, P.G., 1980. *Quantitative Seismology – Theory and Methods*. Volume 1. W. H. Freeman and Co., San Francisco.
- Bashan, A., Bartsch, R., Kantelhardt, J.W. and Havlin, S., 2008. “Comparison of detrending methods for fluctuation analysis”. *Physica A*, Vol. 387, No. 21, pp. 5080-5090.
- Chen, W. and Holm, S., 2004. “Fractional Laplacian time-space models for linear and nonlinear lossy media exhibiting arbitrary frequency power-law dependency”. *Journal of Acoustical Society of America*, Vol. 115, No. 4, pp. 1424-1430.

- Di Benedetto H. and Tatsuoka, F., 1997. "Small strain behavior of geomaterials: modelling of strain rate effects". *Soils and Foundations*, Vol. 37, No. 2, pp. 127–138.
- El Debs, M.K., 2003. *Structural design of circular reinforced concrete pipes (in Portuguese)*. IBTS – Instituto Brasileiro de Telas Soldadas, São Paulo.
- Galhardo, C.E.C., Penna, T.J.P., Argollo de Menezes, M. and Soares, P.P.S., 2009. "Detrended fluctuation analysis of a systolic blood pressure control loop". *New Journal of Physics*, Vol. 11(2009), pp. 103005.
- GO-Associates/Trata Brasil Institute, 2021, *Water losses 2021 (SNIS 2019): challenges for water availability and advancing the efficiency of basic sanitation (in Portuguese)*. Report by Instituto Trata Brasil, São Paulo, Brazil.
- Liu, C., Li, Y., Fang, L., Han, J. and Xu, M., 2017. "Leakage monitoring research and design for natural gas pipelines based on dynamic pressure waves". *Journal of Process Control*, Vol. 50, No. 6, pp. 66-76.
- Ohsaki, Y. and Iwasaki, R., 1973. "On dynamic shear moduli and Poisson's ratios of soil deposits". *Soils and Foundations*, Vol. 13, No. 4, pp. 61–73.
- Pinto, C., 2006. *Basic course in Soil Mechanics (in Portuguese)*. Oficina de Textos, São Paulo.
- Pritz, T., 2004. "Frequency power law of material damping". *Applied Acoustics*, Vol. 65(2004), pp. 1027-1036.
- Proença, M.S., 2019. *Application of the Kelvin-Voigt Constitutive Model and the Finite Element Method to determine the influence of soil properties on the detection of water leakage in underground networks (in Portuguese)*. Master's Thesis, Postgraduate Program in Mechanical Engineering, School of Engineering, São Paulo State University (UNESP), Ilha Solteira, Brazil.
- Proença, M.S., Paschoalini, A.T., Silva, J.C., Souza, A., Obata, D.H.S., Lima, L.P.M. and Boaventura, O.D.Z., 2022. "The Finite Element Method applied in the viscoelastic constitutive model of Kelvin-Voigt for characterization of the soil dynamic response to water leakage simulation". *Journal of the Brazilian Society of Mechanical Sciences and Engineering*, Vol. 44, No. 10, pp. 1-14.
- Scussel, O., Brennan, M.J., Almeida, F.C.L., Muggleton, J.M., Rustighi, E. and Joseph, P.F., 2021. "Estimating the spectrum of leak noise in buried plastic water distribution pipes using acoustic or vibration measurements remote from the leak." *Mechanical Systems and Signal Processing*, Vol. 147, No. 15, pp. 107059–107071.
- SNIS – National Sanitation Information System, 2022, *Thematic Diagnosis: Water and Sewage Services – Technical Water Management (in Portuguese)*. Report of National Secretariat for Environmental Sanitation, Brasília, Brazil.
- Sun, J.I., Goleorkhi, R. and Seed, H.B., 1988, *Dynamic moduli and damping ratios for cohesive soils*. Report by National Science Foundation, University of California at Berkeley, Earthquake Engineering Research Center, California, USA.
- Szabo, T.L., 1994. "Time domain wave equations for lossy media obeying a frequency power law". *Journal of Acoustical Society of America*, Vol. 96, No. 1, pp. 491-500.
- Tsutiya, M.T., 2008, *Water Supply: Management of Water and Electric Energy Losses in Supply Systems – Professional Training Guide: Level 2 (in Portuguese)*. Report for National Secretariat for Environmental Sanitation, Salvador, Brazil.
- Zheng, H., Song, W. and Wang, J., 2008. "Detrended fluctuation analysis of forest fires and related weather parameters". *Physica A*, Vol. 387, No. 8, pp. 2091-2099.

7. RESPONSIBILITY NOTICE

The authors are the only responsible for the printed material included in this paper.